Journal of
Materials Chemistry B

ROYAL SOCIETY
OF CHEMISTRY

PAPER

View Article Online
View Journal

Check for updates

Cite this: DOI: 10.1039/d1tb02012a

In cellulo synthesis of dendrimeric sensors for fluorescence-on imaging of bacterial phagocytosis†

Feng Jiang,[a] Yilong Shi,[b] Xiaoxue Zou,[a] Jiahuai Han[b] and Shoufa Han *[a]

Received 13th September 2021,
Accepted 28th October 2021

DOI: 10.1039/d1tb02012a

rsc.li/materials-b

Methods for optical tracking of pathogen–host interactions are of biomedical significance. We herein have reported a high molecular weight pH sensor (Den-pH) that is assembled in bacteria and then stably trapped in bacteria irrespective of bacterial membrane potentials. Endowed with acidity-triggered red fluorescence, Den-pH allows signal-on tracking of *S. aureus* in phagocytosis by macrophages. Intra-bacterial formation of multifunctional optical probes, which offers the advantage of overcoming the liability of conventional potential-sensitive dyes to dissipate from stressed bacteria, offers a new tool to study stressed pathogens.

Introduction

Pathogenic bacteria remain a major health threat,[1,2] necessitating fluorescent labeling of bacteria to probe host–pathogen interactions. Currently, bacteria are often tagged by fluorescent proteins[3–7] or cationic dyes that accumulate in bacteria driven by negative potentials across the bacterial membrane.[8–12] The former approach requires lengthy genetic manipulation and is often incapable of discerning bacteria engulfed in immune cells from extracellular bacteria. In the latter approach, the cationic dyes are prone to dissipation upon stress or damage inflicted on bacteria, *e.g.* loss of membrane potentials caused by antibacterial effectors.[8] As such, methods that could be used to track stressed bacteria while allowing signal-on imaging of internalized bacteria over extracellular ones offer a simplified and yet robust tool for biomedical investigation.

Phagocytosis by which phagocytes capture and destroy invading pathogens is a key defence mechanism of innate immunity.[13–20] To date, phagocytosis has been indirectly assayed *via* cellular uptake of fluorescein-labelled latex beads or dead bacteria.[21–26] Albeit widely used to label bacteria, small molecular cationic dyes readily dissipate from bacteria upon attenuation of membrane potentials caused by antibacterial effectors during phagocytosis. This limits the use of small molecular imaging agents to track stressed bacteria. Recently, intra-organelle chemical ligation was employed to image mitophagy using a multifunctional optical probe formed in mitochondria. Stably trapped in stressed mitochondria, the *in situ* formed probe enables dual color tracking of stressed mitochondria in mitophagy by acidity-triggered fluorescence upon delivery of mitochondria into acidic autolysosomes.[27] Mitochondria are endosymbionts evolved from an ancient proteobacterium.[28–30] Viable bacteria possess transmembrane potentials critical for normal cell functions, a parameter akin to mitochondrial membrane potentials.[31,32] To date, imaging of bacteria with optical sensors synthesized *in situ* has been largely unexplored.

Staphylococcus aureus (*S. aureus*) is highly pathogenic[33,34] and is associated with multiple diseases such as wound infection[35–38] and infective endocarditis.[39–43] Inspired by intra-organelle chemical ligation used to track stressed mitochondria in mitophagy, we sought to image phagocytosis of *S. aureus via* bacterium-constricted chemical ligation (BCCL) using a pair of conventional potential-sensitive probes, which each alone fails to track bacteria with ablated membrane potentials (Fig. 1). This is operated *via* strain-promoted azide–alkyne cycloaddition (SPAAC) between an azido-containing cationic pH sensor ($^{\mathbf{6AZ}}$**ProRed**) and a dibenzocyclooctyne (DBCO)-conjugated blue-emissive cationic probe ($^{\mathbf{DBCO}}$**Blue-TPP**) (Fig. 1). The *in situ* formed acidity-reporting dendritic probe (Den-pH) is stably trapped in stressed *S. aureus*, enabling fluorescence-on imaging of phagocytosis by sensing pH acidification upon delivery of bacteria into phagosomes in macrophage–*S. aureus* interaction (Fig. 1).

---

[a] State Key Laboratory for Physical Chemistry of Solid Surfaces, Department of Chemical Biology, College of Chemistry and Chemical Engineering, the Key Laboratory for Chemical Biology of Fujian Province, The MOE Key Laboratory of Spectrochemical Analysis & Instrumentation, and Innovation Center for Cell Signaling Network, Xiamen University, Xiamen 361005, China. E-mail: shoufa@xmu.edu.cn

[b] State key Laboratory of Cellular Stress Biology, Innovation Center for Cell Signalling Network, School of Life Sciences, Xiamen University, Xiamen 361005, China

† Electronic supplementary information (ESI) available. See DOI: 10.1039/d1tb02012a

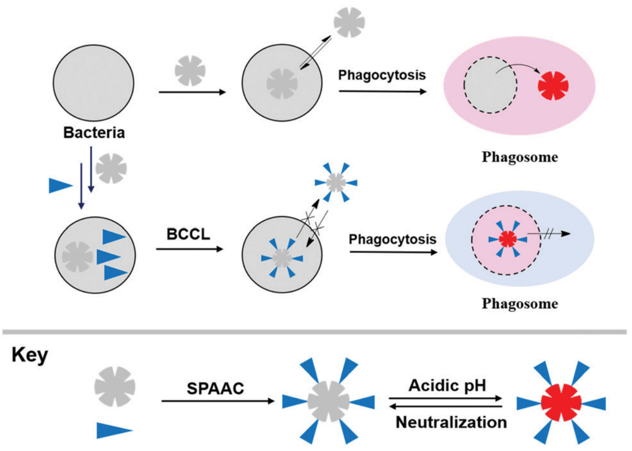

Fig. 1 Schematic of fluorescence-on imaging of bacterial phagocytosis by Den-pH formed in bacteria. $^{\mathrm{6AZ}}$**ProRed** and $^{\mathrm{DBCO}}$**Blue-TPP** that tandemly accumulate in bacteria undergo BCCL to give Den-pH, a hexameric pH-reporting sensor of high molecular weight. Den-pH is stably trapped in bacteria and exhibits turn-on red fluorescence upon internalization of bacteria into acidic phagolysosomes.

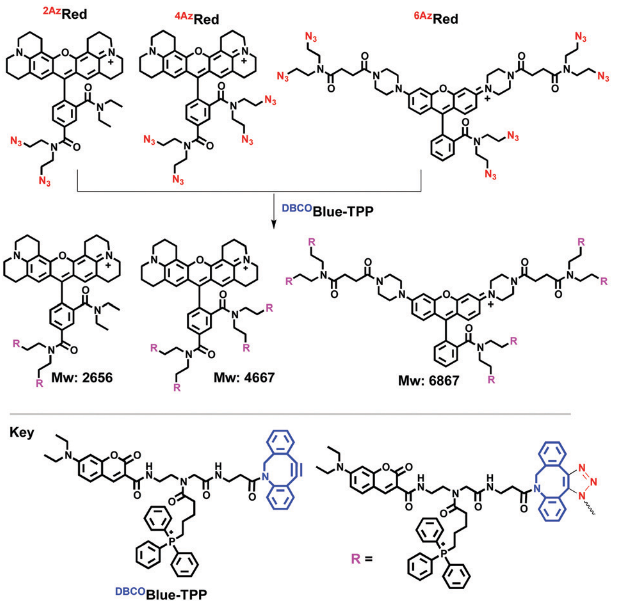

Fig. 2 Model reactions for BCCL: formation of optical probes of different MW in bacteria. Chemical structures and MW of $^{\mathrm{DBCO}}$**Blue-TPP**, $^{\mathrm{2AZ}}$**Red**, $^{\mathrm{4AZ}}$**Red** and $^{\mathrm{6AZ}}$**Red**, and the corresponding divalent, trivalent and hexavalent adducts.

Results and discussion

We first sought to examine whether BCCL could be used to tag bacteria with diminished trans-membrane potentials. As a proof of concept, we developed two sets of chemical probes that (1) selectively accumulate in bacteria, (2) exhibit distinct fluorescence to indicate their retention in bacteria, and (3) contain bio-orthogonal handles for SPAAC. Because cationic rhodamine and triphenylphosphonium (TPP) effectively target bacteria,[8] we synthesized $^{\mathrm{DBCO}}$**Blue-TPP** that contains DBCO for SPAAC, a blue-emissive coumarin, and a TPP moiety. Because diffusion coefficients decrease with increasing molecular mass and to achieve an adduct trappable in *S. aureus*, we also synthesized three cationic rhodamines containing 2, 4 or 6 azido groups, respectively (henceforth referred to as $^{\mathrm{2AZ}}$**Red**, $^{\mathrm{4AZ}}$**Red** and $^{\mathrm{6AZ}}$**Red**) (Fig. 2). These probes were designed to give adducts of varied molecular weight *via* SPAAC with $^{\mathrm{DBCO}}$**Blue-TPP**. *In vitro* reaction of $^{\mathrm{DBCO}}$**Blue-TPP** with $^{\mathrm{2AZ}}$**Red**, $^{\mathrm{4AZ}}$**Red**, or $^{\mathrm{6AZ}}$**Red** gave rise to divalent, tetrameric and hexameric adducts, respectively, as evidenced by mass spectrometry analysis (Fig. S1, ESI†), showing their capability to form adducts of varied molecular weight *via* bio-orthogonal reaction.

To achieve BCCL, we ascertained probe selectivity for bacteria by culturing *S. aureus* with $^{\mathrm{2AZ}}$**Red**, $^{\mathrm{4AZ}}$**Red**, $^{\mathrm{6AZ}}$**Red** or $^{\mathrm{DBCO}}$**Blue-TPP**, independently. We observed bright fluorescence of individual probes inside bacteria (Fig. S2, ESI†), showing their capability to be effectively partitioned in *S. aureus*. These bacterial samples were further treated with carbonyl cyanide m-chlorophenylhydrazone (CCCP) to dissipate the trans-membrane potentials.[44] CCCP caused complete loss of these probes from *S. aureus* (Fig. S3–S5, ESI†), demonstrating the inability of these probes alone to tag *S. aureus* with ablated trans-membrane potential. These results are consistent with the incapability of conventional potential-sensitive dyes to track stressed bacteria. Then, we demonstrated that BCCL of $^{\mathrm{DBCO}}$**Blue-TPP** with $^{\mathrm{2AZ}}$**Red**, $^{\mathrm{4AZ}}$**Red**, or $^{\mathrm{6AZ}}$**Red** efficiently occurred in *S. aureus*, as evidenced by mass spectrometry analysis (Fig. S6, ESI†).

To assess whether high molecular weight (MW) sensors formed in bacteria could be used to track stressed bacteria, we stained *S. aureus* with $^{\mathrm{2AZ}}$**Red**, $^{\mathrm{4AZ}}$**Red**, or $^{\mathrm{6AZ}}$**Red**, and then with $^{\mathrm{DBCO}}$**Blue-TPP**. These bacteria were stressed with CCCP and then visualized for intra-bacterial fluorescence. In sharp contrast to bright red fluorescence that remained in *S. aureus* pre-stained with $^{\mathrm{6AZ}}$**Red**/$^{\mathrm{DBCO}}$**Blue-TPP** after CCCP treatment, $^{\mathrm{2AZ}}$**Red**$^{+}$/$^{\mathrm{DBCO}}$**Blue-TPP**$^{+}$ or $^{\mathrm{4AZ}}$**Red**$^{+}$/**DBCBlue-TPP+** bacteria underwent complete fluorescence loss caused by CCCP (Fig. 3). In addition, *S. aureus* treated with $^{\mathrm{DBCO}}$**Blue-TPP** and azido-free cationic rhodamine that lacks an azido moiety required for SPAAC exhibited fluorescence loss in the presence of CCCP (Fig. S7, ESI†). Taken together, these data show the critical role of higher MW adducts formed *in situ* in fluorescent tagging of stressed *S. aureus*, proving the applicability of BCCL for fluorescence tracking of bacteria without resort to transmembrane potentials.

Having shown that BCCL could be used to tag CCCP-stressed *S. aureus*, it was further employed to track bacteria in phagocytosis. We first introduced a reference signal to pinpoint bacteria by metabolic labelling of the peptidoglycan of *S. aureus* with fluorescein isothiocyanate-conjugated D-lysine (FITC–D-Lys),[8,45] *S. aureus* prelabeled with FITC–D-Lys were cultured with $^{\mathrm{2AZ}}$**Red**, $^{\mathrm{4AZ}}$**Red**, or $^{\mathrm{6AZ}}$**Red**, and then stained with $^{\mathrm{DBCO}}$**Blue-TPP**. The bacteria were washed with PBS, and then co-cultured with bone marrow derived macrophages (BMDMs). Confocal imaging revealed punctate red fluorescence stringently colocalized with FITC–D-Lys in $^{\mathrm{6AZ}}$**Red**$^{+}$/$^{\mathrm{DBCO}}$**Blue-TPP**$^{+}$ bacteria inside macrophages (Fig. S8, ESI†). In contrast, *S. aureus* stained

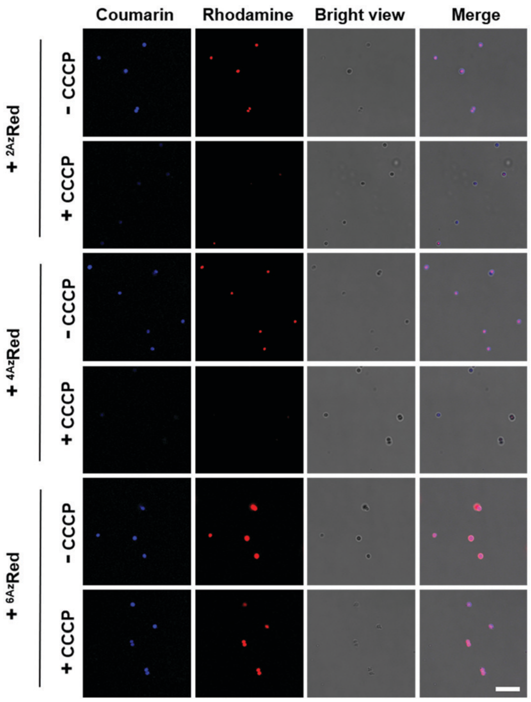

Fig. 3 Effects of the molecular size of optical adducts formed in bacteria on fluorescent tagging of stressed bacteria. *S. aureus* were incubated at 37 °C for 1 h with **^{2AZ}Red** (50 μM), **^{4AZ}Red** (50 μM), or **^{6AZ}Red** (200 μM), and then with **^{DBCO}Blue-TPP** (100 μM, 200 μM, 600 μM) for 1 h. *S. aureus* were washed with phosphate buffered saline (PBS), and then cultured with CCCP (300 μM) for 1 h before confocal microscopic analysis. Scale bar: 6 μm.

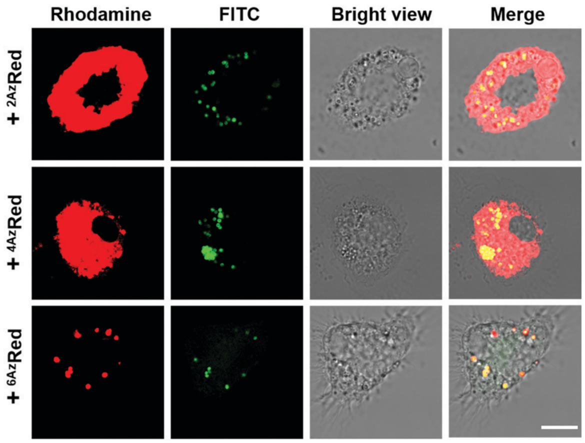

Fig. 4 Effects of molecular size of optical adducts formed in bacteria on tracking stressed bacteria in phagocytosis. *S. aureus* prelabeled with FITC–D-Lys were incubated at 37 °C for 1 h with **^{2AZ}Red** (50 μM), **^{4AZ}Red** (50 μM) and **^{6AZ}Red** (200 μM), and then with **^{DBCO}Blue-TPP** (100 μM, 200 μM, 600 μM) for 1 h. The cells were washed with PBS and then co-cultured with BMDMs for 1 h before confocal microscopic analysis. Scale bar: 15 μm.

with **^{2AZ}Red/^{DBCO}Blue-TPP** or **^{4AZ}Red/^{DBCO}Blue-TPP** gave massive red signals overwhelming punctate green signals of FITC–D-Lys (Fig. 4), reflecting probe leakage from phagocytosed *S. aureus*. These results proved the critical role of higher MW or molecular size of optical sensors formed *in situ* in tracking stressed *S. aureus* in phagocytosis.

Encouraged by the demonstrated applicability of BCCL to track *S. aureus* stressed with CCCP or BMDMs, we set to explore whether BCCL could be employed for signal-on imaging of bacterial phagocytosis. We therefore designed Den-pH that could be synthesized from **^{DBCO}Blue-TPP** and **^{6AZ}ProRed-TPP** (Fig. 5A). **^{6AZ}ProRed-TPP**, integrating a TPP moiety for bacterial targeting and six azido groups for SPAAC, contains X-rhodamine-lactam (ROX-lactam) which is a derivative of ROX suitable for signal-on imaging of acidic lysosomes (Fig. 5A).[46–49] To examine its pH responsiveness, **^{6AZ}ProRed-TPP** was spiked into a buffer of varied pH. Analysis revealed that **^{6AZ}ProRed-TPP** was nonfluorescent at neutral-to-alkaline pH, but exhibited intense red fluorescence in acidic media (Fig. S9A, ESI†), which is consistent with protonation mediated fluorogenic isomerization of ROX-lactam (Fig. 5A). We then synthesized Den-pH *in vitro* and then recorded its fluorescence emission as a function of buffer pH. Den-pH exhibited acidity triggered red fluorescence similar to **^{6AZ}ProRed-TPP** (Fig. 5B). The blue fluorescence of Den-pH was inert to pH alterations (Fig. S9B, ESI†). In addition, there was no detectable FRET effect between the coumarin and rhodamine group of Den-pH (Fig. S9C, ESI†). These results support the potential of Den-pH for signal-on imaging of phagocytosis by acidity-triggered red fluorescence.

To test whether Den-pH could be trapped in stressed bacteria, *S. aureus* were cultured with **^{6AZ}ProRed-TPP** either alone or in combination with **^{DBCO}Blue-TPP**. Both bacterial samples were further treated with CCCP to dissipate transmembrane potentials and then suspended in a buffer of pH 4.0 or pH 7.0. CCCP caused a significant decrease of red fluorescence in **^{6AZ}ProRed-TPP**$^{+}$ *S. aureus*, whereas the red fluorescence in **^{6AZ}ProRed-TPP**$^{+}$/**^{DBCO}Blue-TPP**$^{+}$ (Den-pH) *S. aureus* was largely unaffected (Fig. 6 and Fig. S10, ESI†). In addition, Den-pH synthesized *in vitro* was incapable of staining *S. aureus* (Fig. S11, ESI†). Combined, these results demonstrated that Den-pH formed from intra-bacterial ligation enabled retention of acidity-reporting red fluorescence in CCCP-stressed bacteria.

We then assessed the acidity responsiveness of Den-pH in bacteria by suspending Den-pH^{+} *S. aureus* in a buffer of pH 4.0–8.0. Confocal imaging revealed bright rhodamine fluorescence in bacteria maintained at acidic pH, whereas no fluorescence could be identified in *S. aureus* at pH 8.0–6.0 (Fig. 7A), showing acidity-elicited red fluorescence of Den-pH in live bacteria. Flow cytometry revealed intense red fluorescence displayed within *S. aureus* at acidic pH as compared to that at neutral or alkaline pH (Fig. 7B).

After validating that Den-pH could be trapped in bacteria irrespective of membrane potentials whereby it exhibited acidity-triggered red fluorescence, we were keen to test its performance to track bacterial phagocytosis. *S. aureus* were labeled with FITC–D-Lys and then stained with **^{6AZ}ProRed-TPP/^{DBCO}Blue-TPP** (henceforth referred to as FITC–D-Lys^{+}/Den-pH^{+} *S. aureus*). The bacteria were isolated and then co-cultured with BMDMs. We observed discrete red fluorescence colocalized with green fluorescence of FITC–D-Lys inside

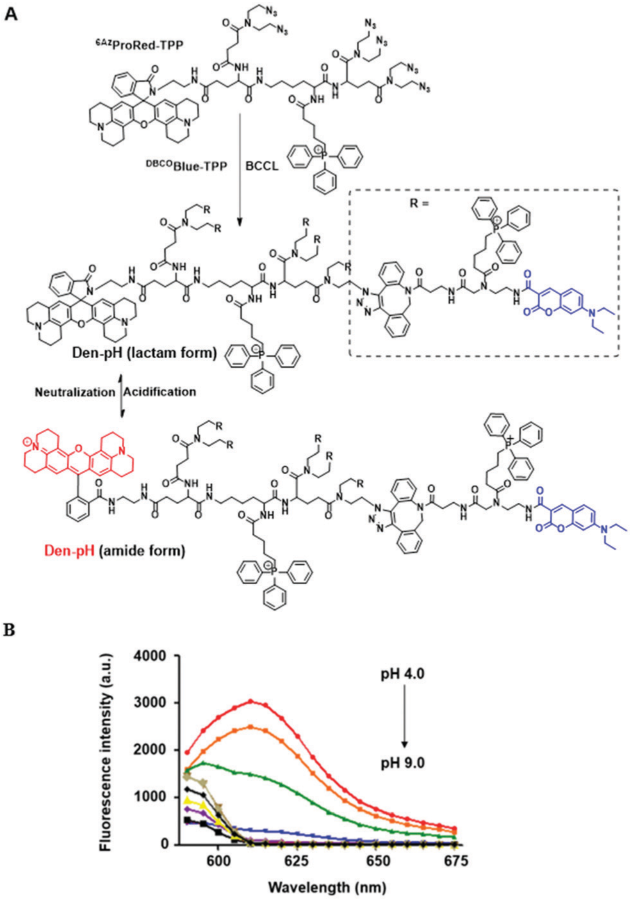

Fig. 5 Optical property of Den-pH. (A) Formation of Den-pH by *in vitro* SPAAC of ^{Az}ProRed-TPP with $^{\mathbf{DBCO}}$**Blue-TPP** and acidity triggered fluorogenic isomerization of Den-pH. (B) pH titration of Den-pH. Fluorescence emission spectra of Den-pH. Den-pH was added to PBS buffer (10 mM) of varied pH (4.0–9.0) to a final concentration of 10 μM, and the solutions were analyzed for fluorescence emission using λ_{ex} = 590 nm.

macrophages (Fig. 8). In contrast, bacteria outside macrophages exhibited bright green fluorescence and null red fluorescence (Fig. 8 and Fig. S12, ESI†). In addition, FITC–D-Lys$^+$ *S. aureus* stained with $^{\mathbf{6AZ}}$**ProRed-TPP** alone gave rise to massive red fluorescence over green fluorescence in BMDMs, reflecting leakage of $^{\mathbf{6AZ}}$**ProRed-TPP** from bacteria to lysosomes (Fig. 8 and Fig. S13, ESI†). In separate experiments we showed that $^{\mathbf{DBCO}}$**Blue-TPP** was located in mitochondria whereas Den-pH was located within the lysosomes of BMDMs (Fig. S14 and Fig. S15, ESI†). These results validate the feasibility of BCCL for fluorescence-on tracking of phagocytosis and the use of Den-pH to differentiate phagocytosed bacteria from unphagocytosed ones.

To consolidate phagosomal acidity-mediated red fluorescence in bacteria, BMDMs loaded with FITC–D-Lys$^+$/Den-pH$^+$ *S. aureus* were treated with Bafilomycin A1 (Baf-A1), a potent ATPase inhibitor, to neutralize phagolysosomal acidic pH.[50,51] In contrast to bright red fluorescence associated with phagocytosed *S. aureus*, Baf-A1 treatment leads to loss of red fluorescence of Den-pH trapped in bacteria (Fig. 9), validating phagolysosomal acidity-elicited red fluorescence of Den-pH in phagocytosis.

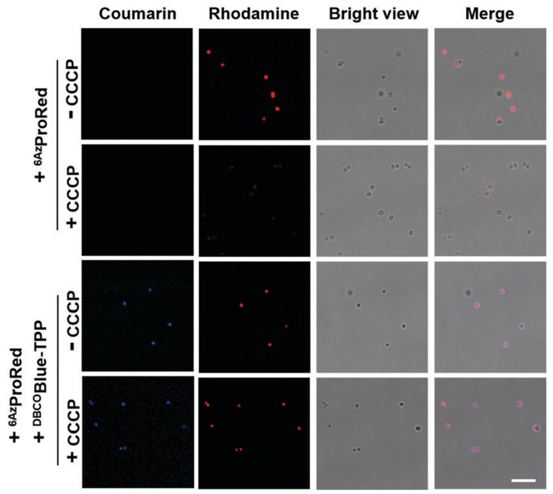

Fig. 6 Den-pH formed in bacteria enables fluorescent tagging of CCCP-stressed *S. aureus*. *S. aureus* were incubated at 37 °C for 1 h with or without $^{\mathbf{DBCO}}$**Blue-TPP** (300 μM), and then with $^{\mathbf{6AZ}}$**ProRed-TPP** (200 μM) for 1 h. The bacteria were maintained in PBS buffer (pH 4.0) containing CCCP (300 μM) for 1 h and then visualized by confocal microscopy. Scale bar: 6 μm.

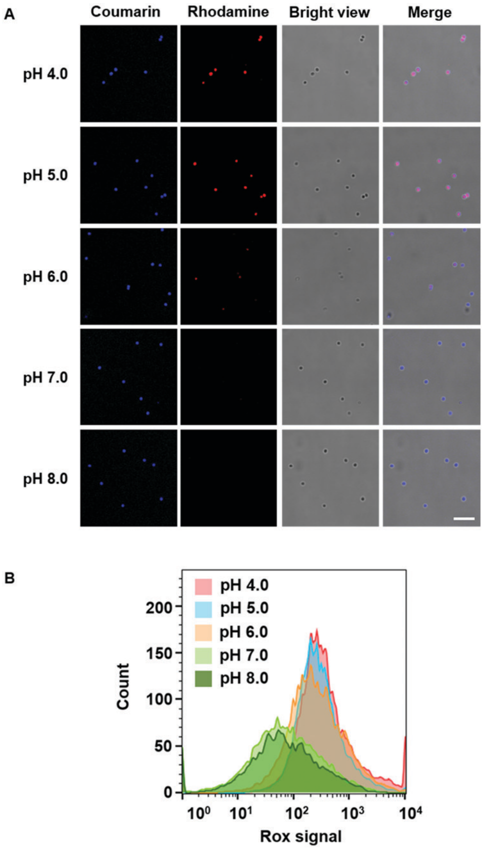

Fig. 7 pH responsiveness of Den-pH in bacteria. *S. aureus* pre-stained with $^{\mathbf{DBCO}}$**Blue-TPP** (300 μM) and $^{\mathbf{6AZ}}$**ProRed-TPP** (200 μM) were resuspended in buffers of pH 4–8 before confocal microscopic analysis (A) or flow cytometry (B). Flow cytometric assays were performed using λ_{ex} =565 nm and λ_{em} = 590–620 nm for rhodamine fluorescence. Scale bar: 6 μm.

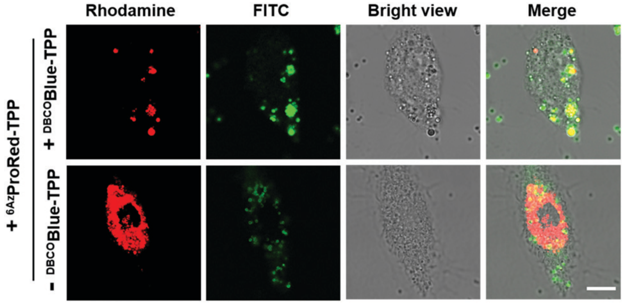

Fig. 8 BCCL enabled fluorescence-on imaging of phagocytosis of *S. aureus* by macrophages. *S. aureus* pre-labeled with FITC–D-Lys were incubated at 37 °C for 1 h with **^{6AZ}ProRed-TPP** (200 μM) and then with or without **^{DBCO}Blue-TPP** (600 μM) for 1 h. The bacteria were harvested, washed and then co-cultured with BMDMs for 1 h before confocal microscopy imaging. Scale bar: 15 μm.

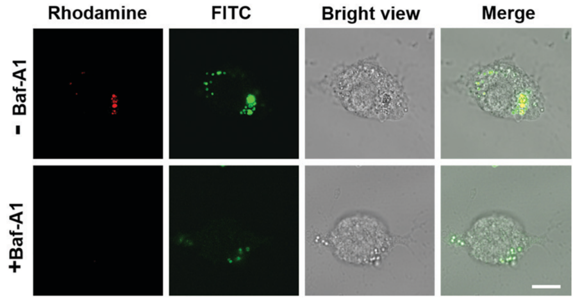

Fig. 9 Effects of phagolysosomal acidity on red fluorescence of Den-pH in phagocytosis. FITC–D-Lys$^+$ *S. aureus* were incubated with **^{6AZ}ProRed-TPP** (200 μM) and then with **^{DBCO}Blue-TPP** (600 μM). The bacteria were co-cultured with BMDMs for 1 h. BMDMs were further treated with or without Baf-A1 (50 nM) for 8 h, and then visualized by confocal microscopy. Scale bar: 10 μm.

Conclusion

Optical tracking of stressed bacteria is valuable to probe pathogen–host interactions where methods that could be used to pinpoint phagocytosed bacteria are of biomedical significance. We herein report bacteria-confined chemical ligation (BCCL) for signal-on imaging of *S. aureus* upon phagocytosis. BCCL employs two conventional small molecular probes, which each alone fails to track stressed bacteria, to form Den-pH, a dendritic pH sensor of high molecular weight that could be stably trapped in bacteria without resort to bacterial membrane potentials. Uptake of Den-pH-loaded *S. aureus* into phagosomes leads to acidity triggered red fluorescence whereas unphagocytosed bacteria exhibit blue fluorescence. The signal-on imaging of phagocytosis shows the utility of BCCL for obtaining multifunctional optical sensors for tracking stressed bacteria, representing a new perspective from which to study stressed pathogens.

Experimental

Materials and methods

LysoTracker Blue DND 22 was purchased from Invitrogen. Bafilomycin A1 (Baf-A1) was purchased from Sigma. 5-Carboxy-X-rhodamine (5-ROX) was obtained from Biolumi-nor, Xiamen. FITC–D-Lys and ROX-EDA were synthesized following a reported procedure.[8] TPP-NHS was synthesized following a reported procedure.[52] Bis(2-azidoethyl)amine, **0AzRed** and **^{2AZ}Red** were synthesized following a reported procedure.[27] Compound **9** was prepared following a reported procedure.[53] All other reagents were purchased from Alfa Aesar. NMR spectra were recorded on a Bruker instrument using tetramethyl silane as the internal reference. Mass analysis was performed on Bruker En Apex ultra 7.0T FT-MS.

The fluorescent spectra were collected with SpectraMax M5. Confocal microscopy imaging was performed on Leica SP8 using the following filters: λ_{ex}@552 nm and λ_{em}@565–650 nm for RB and ROX signals; λ_{ex}@488 nm and λ_{em}@500–530 nm for the FITC signal; and λ_{ex}@405 nm and λ_{em}@430–4800 nm for coumarin and LysoTracker blue. The images of merged fluorescence were processed using LAS X. Graphs were generated with Graphpad Prism 7.

General procedure for bacterial labelling: *S. aureus* were grown at 37 °C in LB medium until the OD_{600} reached 0.6 and then the culture was diluted to $OD_{600} \sim 0.3$ with fresh LB medium spiked with indicated optical probes. *S. aureus* were harvested by centrifugation, washed with PBS three times, and then resuspended in LB medium containing another probe for BCCL. These BCCL$^+$ cells were collected by centrifugation and rinsed three times with PBS for further applications.

Synthetic procedures of ^{6AZ}ProRed-TPP (Scheme S1, ESI†)

Synthesis of compound 1. To a flask containing *N*,*N*-dimethylformamide (DMF, 5 mL), TPP-NHS (460 mg, 1 mmol) and *N*^{6}-[(1,1-dimethylethoxy)carbonyl]-L-lysine (369 mg, 1.5 mmol) was added triethylamine (TEA) (404 mg, 4 mmol). The mixture was stirred at room temperature for 3 h and then concentrated *in vacuo*. The residue was dissolved in CH_2Cl_2 (10.0 mL). The organic solution was washed with aqueous hydrochloric acid (1 M, 3 × 10.0 mL) and saturated sodium chloride (10.0 mL), dehydrated with anhydrous Na_2SO_4, and then concentrated. The residue was subjected to silica gel chromatography using CH_2Cl_2/MeOH (10 : 1) as the eluent to yield compound **1** in 90% yield (530.0 mg). ^{1}H NMR (500 MHz, DMSO) δ 12.50 (s, 1H), 8.11 (d, J = 7.7 Hz, 1H), 7.89 (ddd, J = 6.7, 5.2, 2.1 Hz, 3H), 7.84–7.72 (m, 12H), 6.77 (t, J = 5.4 Hz, 1H), 4.09 (td, J = 8.4, 5.1 Hz, 1H), 3.61 (dd, J = 15.9, 14.0 Hz, 2H), 2.84 (tt, J = 8.6, 4.3 Hz, 2H), 2.19 (t, J = 7.1 Hz, 2H), 1.70 (dq, J = 14.4, 7.1 Hz, 2H), 1.61 (dd, J = 19.9, 6.3 Hz, 1H), 1.57–1.44 (m, 3H), 1.36 (s, 9H), 1.31 (dd, J = 14.5, 7.2 Hz, 2H), 1.21 (dd, J = 15.0, 7.8 Hz, 2H). ^{13}C NMR (126 MHz, DMSO) δ 173.67, 171.74, 155.57, 134.89, 134.87, 133.61, 133.53, 130.29, 130.19, 118.86, 118.18, 77.34, 51.74, 34.00, 30.68, 29.06, 28.26, 26.21, 26.07, 22.78, 21.31, 20.34, 19.94. MS (ES$^+$) calcd for $C_{34}H_{44}N_2O_5P^+$ (M^+) *m*/*z* 591.2982; found: 591.1.

Synthesis of compound 2. To the solution of *N*-[(1,1-dimethylethoxy) carbonyl]-L-glutamic acid (335 mg, 1.36 mmol) in DMF (5.0 mL) were added 4-(4,6-dimethoxy-1,3,5-triazin-2-yl)-4-methylmorpholinium chloride (DMTMM, 1.12 g, 4.08 mmol) and bis(2-azidoethyl) amine (626.0 mg, 4.08 mmol). The reaction solution was stirred for 5 h at room temperature and then concentrated. The residue was dissolved in CH_2Cl_2 (15.0 mL). The resultant organic solution was washed with aqueous hydrochloric acid (1 M, 3 × 10.0 mL), extracted with saturated aqueous sodium bicarbonate (3 × 10.0 mL), dried with anhydrous Na_2SO_4, and then concentrated. The residue was purified by silica gel chromatography using petroleum ether/ethyl acetate (1 : 1) as the eluent to afford compound **2** in 92% yield (650.0 mg). ^{1}H NMR (500 MHz, $CDCl_3$) δ 5.78 (s, 1H), 5.48 (d, J = 8.6 Hz, 1H), 4.64 (t, J = 8.7 Hz, 1H), 4.14 (dd, J = 9.3, 5.8 Hz, 1H), 3.79 (dd, J = 20.2, 12.1 Hz, 1H), 3.64–3.48 (m, 11H), 3.46–3.39 (m, 1H), 3.31 (dd, J = 13.2, 5.8 Hz, 1H), 2.68–2.53 (m, 1H), 2.42 (d, J = 16.9 Hz, 1H), 2.11 (d, J = 23.4 Hz, 1H), 1.67 (t, J = 12.0 Hz, 1H), 1.42 (s, 9H). ^{13}C NMR (126 MHz, $CDCl_3$) δ 173.82, 172.78, 156.08, 100.08, 80.25, 50.28, 49.88, 49.67, 49.56, 49.29, 48.07, 47.97, 46.99, 46.51, 28.60, 28.34. MS (ES^+) calcd for $C_{18}H_{32}N_{15}O_4$ (M + H) m/z 522.276, found: 522.4.

Synthesis of compound 4. Compound **2** (572.0 mg, 0.92 mmol) was dissolved in CH_2Cl_2 (12.0 mL) containing trifluoroacetic acid (TFA, 4.0 mL). The mixture was stirred at room temperature for 1 h and then concentrated *in vacuo*. The residue was dissolved in CH_2Cl_2 (30.0 mL). The organic solution was washed with saturated aqueous solution of $NaHCO_3$ (30.0 mL), dehydrated with Na_2SO_4, and then concentrated to afford crude product compound **3**. To the solution of compound **1** (494 mg, 0.83 mmol) in CH_2Cl_2 (20.0 mL) were added 1-(3-dimethylaminopropyl)-3-ethylcarbodiimide hydrochloride (EDC) (240 mg, 1.25 mmol) and *N*-hydroxysuccinimide (NHS, 144 mg, 1.25 mmol). The reaction mixture was stirred at room temperature for 1.5 h, followed by the addition of crude compound **3** and TEA (253 mg, 2.51 mmol). The reaction mixture was stirred at room temperature for 8 h and then washed with aqueous hydrochloric acid (1 M, 3 × 20.0 mL). The organic phase was extracted with saturated aqueous sodium bicarbonate (3 × 20.0 mL), dried over anhydrous sodium sulfate, and then concentrated by rotary evaporation. The residue was purified by Al_2O_3 chromatography using CH_2Cl_2/MeOH (75 : 1) as the eluent to afford compound **4** in 88% yield (731.0 mg). ^{1}H NMR (500 MHz, $CDCl_3$) δ 9.27 (d, J = 7.1 Hz, 1H), 7.81–7.74 (m, 9H), 7.72–7.64 (m, 6H), 4.97 (s, 1H), 4.79 (d, J = 8.3 Hz, 1H), 4.40 (d, J = 3.5 Hz, 1H), 4.16–4.01 (m, 1H), 3.71 (s, 2H), 3.62 (dd, J = 12.8, 7.1 Hz, 2H), 3.57–3.42 (m, 10H), 3.33–3.20 (m, 1H), 3.15 (dd, J = 11.9, 5.4 Hz, 1H), 3.12–2.94 (m, 3H), 2.73 (dd, J = 33.1, 17.7 Hz, 2H), 2.48 (d, J = 15.8 Hz, 2H), 2.05 (s, 1H), 2.00–1.74 (m, 6H), 1.69 (s, 1H), 1.46 (d, J = 34.5 Hz, 2H), 1.37 (s, 9H), 1.31–1.16 (m, 1H). ^{13}C NMR (126 MHz, $CDCl_3$) δ 173.08, 172.93, 172.91, 156.14, 135.14, 133.74, 133.66, 130.66, 130.57, 130.47, 118.83, 118.15, 78.85, 54.12, 50.55, 50.34, 49.29, 48.85, 48.73, 47.96, 47.78, 46.82, 46.45, 34.05, 32.04, 29.22, 28.62, 28.52, 27.40, 23.39, 21.06. MS (ES^+) calcd for $C_{47}H_{65}N_{17}O_6P^+$ (M^+) m/z 994.504, found: 994.6.

Synthesis of compound 6. Compound **4** (600.0 mg, 0.60 mmol) was dissolved in CH_2Cl_2 (18.0 mL) containing TFA (6.0 mL). The mixture was stirred at room temperature for 1 h and then concentrated *in vacuo*. The residue was dissolved in CH_2Cl_2 (30.0 mL). The organic solution was washed with saturated aqueous solution of $NaHCO_3$ (30.0 mL), dehydrated with Na_2SO_4, and then concentrated to afford crude product compound **5**. To the solution of *N*-[(1,1-dimethylethoxy) carbonyl]-5-methyl ester-L-glutamic acid (204 mg, 0.78 mmol) in CH_2Cl_2 (10.0 mL) were added EDC (231 mg, 1.21 mmol) and NHS (138 mg, 1.21 mmol). The reaction mixture was stirred at room temperature for 1 h, followed by the addition of crude compound **5** and TEA (182 mg, 1.80 mmol). The reaction mixture was stirred at room temperature overnight and then washed with aqueous hydrochloric acid (1 M, 2 × 10.0 mL). The organic phase was extracted with saturated aqueous sodium bicarbonate (2 × 10.0 mL), dried over anhydrous sodium sulfate, and then concentrated by rotary evaporation. The residue was purified by Al_2O_3 chromatography using CH_2Cl_2/MeOH (50 : 1) as the eluent to afford compound **6** in 80% yield (549.0 mg). ^{1}H NMR (500 MHz, $CDCl_3$) δ 9.28 (s, 1H), 8.06 (s, 1H), 7.79 (d, J = 5.2 Hz, 9H), 7.70 (s, 6H), 5.73 (d, J = 7.1 Hz, 1H), 4.85 (t, J = 8.3 Hz, 1H), 4.39 (t, J = 13.3 Hz, 1H), 4.27 (s, 1H), 4.11 (d, J = 15.1 Hz, 1H), 3.88 (s, 1H), 3.60 (d, J = 5.8 Hz, 4H), 3.57 (s, 3H), 3.52 (dd, J = 14.9, 7.7 Hz, 7H), 3.45–3.36 (m, 2H), 3.34–3.24 (m, 2H), 3.24–3.10 (m, 2H), 2.95 (s, 2H), 2.78 (s, 1H), 2.58 (d, J = 44.4 Hz, 2H), 2.42–2.34 (m, 2H), 2.11 (s, 2H), 2.00 (s, 2H), 1.91 (s, 1H), 1.75 (s, 4H), 1.61 (s, 2H), 1.45 (s, 2H), 1.36 (s, 9H), 1.25 (d, J = 16.1 Hz, 1H). ^{13}C NMR (126 MHz, $CDCl_3$) δ 173.99, 173.88, 172.69, 172.53, 171.55, 155.38, 135.11, 133.67, 133.59, 130.58, 130.48, 118.67, 117.98, 79.10, 54.30, 53.35, 51.61, 50.38, 50.14, 49.19, 48.96, 48.39, 47.87, 47.65, 46.64, 46.37, 37.94, 34.21, 30.48, 30.14, 29.08, 28.36, 28.02, 27.92, 26.62, 26.49, 22.52, 21.79, 21.38, 21.29. MS (ES^+) calcd for $C_{53}H_{74}N_{18}O_9P^+$ (M^+) m/z 994.504, found: 994.6.

Synthesis of compound 7. Compound **6** (380.0 mg, 0.33 mmol) was dissolved in CH_2Cl_2 (9.0 mL) containing TFA (3.0 mL). The mixture was stirred at room temperature for 1 h and then concentrated *in vacuo*. The residue was dissolved in CH_2Cl_2 (20.0 mL). The organic solution was washed with saturated aqueous solution of $NaHCO_3$ (30.0 mL) and dehydrated with Na_2SO_4. To the above organic solution were added succinic anhydride (40 mg, 0.40 mmol), TEA (74 mg, 0.73 mmol) and 4-dimethylaminopyridine (DMAP, 40 mg, 0.33 mmol). The solution was stirred at room temperature overnight and then washed with aqueous hydrochloric acid (1 M, 2 × 20.0 mL). The organic layer was dried with Na_2SO_4. To the above organic solution were added DMTMM (92 mg, 0.33 mmol) and bis(2-azidoethyl) amine (155.0 mg, 1.0 mmol). The reaction solution was stirred overnight at room temperature and then concentrated. The residue was dissolved in CH_2Cl_2 (15.0 mL). The solution was washed with aqueous hydrochloric acid (1 M, 2 × 10.0 mL), extracted with saturated aqueous sodium bicarbonate (2 × 10.0 mL), dried with anhydrous Na_2SO_4, and then concentrated. The residue was purified by Al_2O_3 chromatography using CH_2Cl_2/MeOH (50 : 1) as the eluent to afford compound **7** in 62% yield (264.0 mg). ^{1}H NMR (500 MHz, $CDCl_3$) δ 9.18 (s, 1H), 8.08 (s, 1H), 7.86–7.66 (m, 15H), 7.21 (d, J = 8.0 Hz, 1H), 4.83 (dd, J = 22.1, 13.7 Hz, 1H), 4.61 (dd, J = 8.7, 4.5 Hz, 1H), 4.23 (s, 1H), 4.07 (dd, J = 17.7, 12.2 Hz, 1H), 3.75 (t, J = 13.6 Hz, 1H), 3.69–3.58 (m, 5H), 3.57 (s, 3H), 3.56–3.42 (m, 9H), 3.39 (dd, *J* = 12.4, 6.2 Hz, 1H), 3.35–3.28 (m, 1H), 3.27–3.01 (m, 3H), 2.94–2.67 (m, 5H), 2.59 (dd, *J* = 21.7, 16.5 Hz, 4H), 2.53–2.37 (m, 4H), 2.37–2.18 (m, 3H), 2.17–2.03 (m, 1H), 1.94 (s, 3H), 1.63 (dd, *J* = 64.0, 49.6 Hz, 6H), 1.40 (d, *J* = 30.9 Hz, 2H), 1.37–1.16 (m, 3H). ^{13}C NMR (126 MHz, $CDCl_3$) δ 177.80, 173.36, 172.90, 172.82, 168.04, 135.34, 135.32, 133.71, 133.63, 130.70, 130.60, 118.68, 117.99, 54.69, 53.25, 51.69, 50.63, 50.53, 50.29, 49.33, 49.07, 48.43, 48.40, 47.97, 47.76, 46.71, 46.41, 38.12, 34.31, 31.37, 30.32, 28.85, 28.46, 28.19, 27.80, 26.51, 26.39, 23.62, 22.49, 22.25, 21.84, 21.56. MS (ES^+) calcd for $C_{56}H_{77}N_{25}O_9P^+$ (M^+) *m/z* 1274.607, found: 1274.9.

Synthesis of ^{6AZ}ProRed-TPP

To the solution of compound **7** (120.0 mg, 0.09 mmol) in tetrahydrofuran (THF, 4.0 mL) was added aqueous solution of NaOH (8 mg, 1.0 mL). The solution was stirred at room temperature for 4 h and then neutralized with aqueous hydrochloric acid (1 M). The reaction mixture was concentrated *in vacuo*. The residue was dissolved in DMF (5 mL). To the above organic solution were added DMTMM (64 mg, 23.7 mmol) and ROX-EDA (101 mg, 0.19 mmol). The reaction solution was stirred for 8 h at room temperature and then concentrated. The residue was dissolved in CH_2Cl_2 (10.0 mL) and then washed with H_2O (10.0 mL). Then the organic phase was extracted with saturated aqueous sodium bicarbonate (2 × 10.0 mL). The organic phase was dried with anhydrous Na_2SO_4 and then concentrated. The residue was purified by silica gel chromatography using ethyl acetate/CH_3OH/TEA (5 : 1 : 0.05) as the eluent to afford compound **^{6AZ}ProRed-TPP** in 60% yield (100.0 mg). ^{1}H NMR (500 MHz, $CDCl_3$) δ 7.91–7.62 (m, 16H), 7.43 (dd, *J* = 16.0, 13.1 Hz, 2H), 7.11–6.97 (m, 1H), 5.97 (s, 2H), 4.81 (dd, *J* = 18.0, 9.4 Hz, 1H), 4.46–4.15 (m, 1H), 3.75–3.57 (m, 6H), 3.53–3.38 (m, 10H), 3.36–3.21 (m, 5H), 3.10 (d, *J* = 25.3 Hz, 10H), 2.88 (s, 5H), 2.68–2.53 (m, 3H), 2.53–2.25 (m, 10H), 2.19 (dd, *J* = 18.2, 10.4 Hz, 2H), 2.09 (d, *J* = 16.3 Hz, 2H), 2.02 (s, 4H), 1.92 (d, *J* = 7.8 Hz, 2H), 1.86 (d, *J* = 31.6 Hz, 7H), 1.75 (d, *J* = 7.0 Hz, 3H), 1.62–1.51 (m, 2H), 1.39 (dd, *J* = 19.2, 8.5 Hz, 2H), 1.33–1.26 (m, 5H), 1.23–1.16 (m, 3H). ^{13}C NMR (126 MHz, $CDCl_3$) δ 172.87, 172.81, 172.80, 172.78, 148.22, 143.70, 135.22, 135.07, 133.65, 133.57, 132.65, 130.56, 130.51, 130.41, 129.99, 129.76, 127.97, 124.24, 124.01, 122.72, 118.79, 117.49, 107.71, 104.88, 50.46, 50.38, 50.32, 50.29, 50.19, 50.13, 50.11, 50.10, 49.86, 49.84, 49.40, 49.26, 49.23, 49.19, 49.00, 48.97, 47.88, 47.85, 47.76, 47.74, 47.70, 46.82, 46.71, 46.65, 46.37, 46.34, 37.09, 35.91, 34.46, 31.91, 31.90, 31.43, 31.39, 30.18, 30.02, 29.76, 29.69, 29.62, 29.51, 29.36, 29.31, 29.27, 29.13, 28.30, 27.17, 25.57, 22.68, 21.90, 21.39, 21.20, 14.12. HRMS (ES^+) calcd for $C_{89}H_{109}N_{29}O_{10}P^+$ (M^+) *m/z* 1775.8678, found 1775.8699.

Synthesis of ^{2AZ}Red (Scheme S2A, ESI†)

To a solution of 5-ROX (100 mg, 0.19 mmol) in DMF (4.0 mL) were added DMTMM (126.0 mg, 0.47 mmol) and bis(2-azidoethyl)amine (72.5 mg, 0.47 mmol). The reaction solution was stirred for 8 h at room temperature and then concentrated. The residue was dissolved in CH_2Cl_2 (10.0 mL) and then washed with aqueous hydrochloric acid (1 M, 2 × 10.0 mL). The organic phase was extracted with saturated aqueous sodium bicarbonate (2 × 10.0 mL). The organic layer was dried over anhydrous sodium sulfate, and then concentrated by rotary evaporation. The residue was purified by silica gel chromatography using CH_2Cl_2/MeOH (20 : 1) as the eluent to afford **^{4AZ}Red** (124.0 mg, 85%). ^{1}H NMR (500 MHz, $CDCl_3$) δ 7.76 (d, *J* = 6.2 Hz, 2H), 7.38 (d, *J* = 8.0 Hz, 1H), 6.79 (s, 2H), 3.84–3.68 (m, 5H), 3.53 (t, *J* = 24.6 Hz, 11H), 3.32 (d, *J* = 49.6 Hz, 4H), 3.08 (s, 2H), 3.04–2.92 (m, 4H), 2.75 (d, *J* = 13.9 Hz, 4H), 2.21 (s, 2H), 2.07 (s, 4H), 2.02–1.90 (m, 4H). ^{13}C NMR (126 MHz, $CDCl_3$) δ 170.95, 168.89, 152.00, 151.43, 137.50, 136.28, 132.25, 130.88, 128.56, 126.85, 123.88, 112.92, 105.31, 51.14, 50.61, 49.25, 48.89, 48.65, 43.00, 27.46, 20.69, 19.91, 19.74. HRMS (ES^+) calcd for $C_{41}H_{45}N_{16}O_3^+$ (M^+) *m/z* 809.3855, found 806.3860.

Synthetic procedures of ^{4AZ}Red (Scheme S2B, ESI†)

Synthesis of compound 10. To the solution of compound **9** (200.0 mg, 0.30 mmol) in CH_2Cl_2 (5.0 mL) were added DMTMM (320 mg, 1.20 mmol) and bis(2-azidoethyl) amine (70.0 mg, 0.46 mmol). The reaction solution was stirred for 48 h at room temperature and then concentrated. The residue was dissolved in CH_2Cl_2 (15.0 mL) and the resultant organic solution was washed with aqueous hydrochloric acid (1 M, 3 × 10.0 mL). The organic phase was washed with saturated aqueous sodium bicarbonate (3 × 10.0 mL). The organic phase was dried with anhydrous Na_2SO_4 and then concentrated. The residue was purified by silica gel chromatography using CH_2Cl_2/MeOH (10 : 1) as the eluent to afford compound **10** in 30% yield (72.0 mg). ^{1}H NMR (500 MHz, $CDCl_3$) δ 7.69 (ddd, *J* = 29.8, 15.0, 7.3 Hz, 3H), 7.50–7.28 (m, 5H), 6.95 (s, 2H), 3.91–3.53 (m, 16H), 3.34 (s, 3H), 3.05 (s, 2H), 2.38–1.93 (m, 3H), 1.46 (s, 18H). ^{13}C NMR (126 MHz, $CDCl_3$) δ 169.64, 158.01, 157.12, 156.49, 154.45, 136.00, 132.51, 130.53, 129.69, 129.65, 128.30, 115.56, 114.74, 97.24, 80.77, 48.84, 48.54, 48.31, 47.03, 42.56, 28.37. MS (ES^+) calcd for $C_{42}H_{52}N_{11}O_6^+$ (M^+) *m/z* 806.410, found 806.7.

Synthesis of ^{6AZ}Red. Compound **10** (60 mg, 0.07 mmol) was dissolved in CH_2Cl_2 (3.0 mL) containing TFA (1.0 mL). The mixture was stirred at room temperature for 1 h and then concentrated *in vacuo*. The residue was dissolved in CH_2Cl_2 (10.0 mL). The organic solution was washed with saturated aqueous solution of $NaHCO_3$ (15.0 mL) and dehydrated with Na_2SO_4. To the above organic solution were added succinic anhydride (20 mg, 0.20 mmol), TEA (30 mg, 0.30 mmol) and DMAP (23 mg, 0.19 mmol). The solution was stirred at room temperature overnight and then washed with aqueous hydrochloric acid (1 M, 2 × 20.0 mL). The organic layer was dried with Na_2SO_4. To the above organic solution were added DMTMM (80 mg, 0.30 mmol) and bis(2-azidoethyl) amine (46.0 mg, 0.30 mmol). The reaction solution was stirred overnight at room temperature and then concentrated. The residue was dissolved in CH_2Cl_2 (15.0 mL) and washed with aqueous hydrochloric acid (1 M, 2 × 10.0 mL). Then the organic phase was extracted with saturated aqueous sodium bicarbonate (2 × 10.0 mL). The organic phase was dried with anhydrous Na_2SO_4 and then concentrated. The residue was purified by

Al_2O_3 chromatography using CH_2Cl_2/MeOH (50 : 1) as the eluent to afford **^{6AZ}Red** in 62% yield (264.0 mg). ^{1}H NMR (500 MHz, $CDCl_3$) δ 7.89–7.57 (m, 3H), 7.37 (d, J = 17.5 Hz, 5H), 6.98 (s, 2H), 3.91 (dd, J = 97.4, 45.2 Hz, 14H), 3.60 (t, J = 46.0 Hz, 15H), 3.33 (s, 4H), 3.07 (s, 2H), 2.71 (d, J = 27.3 Hz, 7H), 1.96 (s, 6H). ^{13}C NMR (126 MHz, $CDCl_3$) δ 172.60, 171.12, 169.57, 157.99, 157.05, 156.55, 135.91, 132.48, 130.62, 129.76, 129.53, 128.29, 115.27, 114.72, 97.28, 49.98, 49.38, 48.81, 48.51, 48.40, 48.16, 46.74, 46.58, 44.30, 42.66, 40.65, 29.67, 28.12, 28.09. HRMS (ES^+) calcd for $C_{48}H_{58}N_{25}O_6^+$ (M^+) m/z 1080.4996, found 1080.5014.

***In vitro* SPAAC of ^{4AZ}Red and ^{DBCO}Blue-TPP.** To a flask containing CH_3OH (0.2 mL) were added **^{4AZ}Red** (5.0 mg, 0.006 mmol) and **^{DBCO}Blue-TPP** (36.0 mg, 0.037 mmol). The reaction solution was stirred for 3 h at room temperature and then analyzed by MS. MALDI-TOF MS. calcd for $C_{277}H_{281}N_{36}O_{27}P_4^{5+}$ (M^{5+}) m/z 933.814, found 933.801.

***In vitro* SPAAC of ^{6AZ}Red and ^{DBCO}Blue-TPP.** To a flask containing CH_3OH (0.2 mL) were added **^{6AZ}Red** (5.0 mg, 0.005 mmol) and **^{DBCO}Blue-TPP** (40.0 mg, 0.041 mmol). The reaction solution was stirred for 3 h at room temperature and then analyzed by MS. MALDI-TOF MS calcd for $C_{402}H_{412}N_{55}O_{42}P_6^{7+}$ (M^{7+}) m/z 981.576, found 981.498.

***In vitro* SPAAC of ^{6AZ}ProRed-TPP and ^{DBCO}Blue-TPP.** To a flask containing CH_3OH (0.2 mL) were added **^{6AZ}ProRed-TPP** (5.0 mg, 0.003 mmol) and **^{DBCO}Blue-TPP** (25.0 mg, 0.026 mmol). The reaction solution was stirred for 3 h at room temperature and then analyzed by MS. MALDI-TOF MS calcd for $C_{443}H_{463}N_{59}O_{46}P_7^{7+}$ (M^{7+}) m/z 1080.914, found 1080.762.

SPAAC of ^{2AZ}Red and ^{DBCO}Blue-TPP in *S. aureus*. *S. aureus* were grown in LB medium containing **^{2AZ}Red** (50 μM) for 60 min, and then cultured with **^{DBCO}Blue-TPP** (100 μM) for 1 h in LB medium. These cells were crashed using an ultrasonic crasher for 15 min, and then analyzed by MS. MALDI-TOF MS calcd for $C_{159}H_{165}N_{20}O_{15}P_2^{3+}$ (M^{3+}) m/z 885.407, found 885.369.

SPAAC of ^{4AZ}Red and ^{DBCO}Blue-TPP in *S. aureus*. *S. aureus* were grown in LB medium containing **^{4AZ}Red** (50 μM) for 60 min, and then cultured with **^{DBCO}Blue-TPP** (200 μM) for 1 h in LB medium. These cells were crashed using an ultrasonic crasher for 15 min, and then analyzed by MS. MALDI-TOF MS calcd for $C_{277}H_{281}N_{36}O_{27}P_4^{5+}$ (M^{5+}) m/z 933.814, found 933.856.

SPAAC of ^{4AZ}Red and ^{DBCO}Blue-TPP in *S. aureus*. *S. aureus* were grown in LB medium containing **^{6AZ}Red** (200 μM) for 60 min, and then cultured with **^{DBCO}Blue-TPP** (600 μM) for 1 h in LB medium. These cells were crashed using an ultrasonic crasher for 15 min, and then analyzed by MS. MALDI-TOF MS calcd for $C_{402}H_{412}N_{55}O_{42}P_6^{7+}$ (M^{7+}) m/z 981.576, found 982.168.

pH titration. An aliquot of **^{6AZ}ProRed-TPP** stock solution was added to a series of phosphate buffered saline solutions (PBS, 10 mM) containing dimethyl sulfoxide (DMSO, 30% v/v) of pH 4.0, 4.5, 5.0, 5.5, 6.0, 6.5, 7.0, 7.5, 8.0, 8.5, and 9.0 to a final concentration of 10 μM. In parallel, the adduct of **^{6AZ}ProRed-TPP/^{DBCO}Blue-TPP** (Den-pH) was added to phosphate buffered saline (PBS) (10 mM) containing 30% DMSO (pH: 4.0, 4.5, 5.0, 5.5, 6.0, 6.5, 7.0, 7.5, 8.0, 8.5, 9.0) to a final concentration of 10 μM. Fluorescence emission of these samples was recorded using λ_{ex} = 430 nm or λ_{ex} = 585 nm. pH titration curves were plotted using fluorescence emission of coumarin (I_{475} nm) or ROX (I_{610} nm) over pH.

Intramolecular FRET of the adduct from ^{6AZ}ProRed-TPP and ^{DBCO}Blue-TPP *in vitro*. The adduct of **^{6AZ}ProRed-TPP/^{DBCO}Blue-TPP** (Den-pH) was added to phosphate buffered saline (PBS) (10 mM) containing 30% DMSO (pH: 4.0, 4.5, 5.0, 5.5, 6.0, 6.5, 7.0, 7.5, 8.0, 8.5, 9.0) to a final concentration of 10 μM. Fluorescence emission of these samples was recorded using λ_{ex} = 430 nm. pH titration curves were plotted using fluorescence emission of coumarin (I_{475} nm) or ROX (I_{610} nm) over pH.

Probe selectivity for *S. aureus*. *S. aureus* were grown in LB medium containing **^{2AZ}Red** (50 μM), **^{4AZ}Red** (50 μM), **^{6AZ}Red** (200 μM), or **^{DBCO}Blue-TPP** (50 μM) for 60 min. These cells were washed with PBS and then analyzed by confocal fluorescence microscopy.

Tagging stressed bacteria *via* BCCL with ^{0Az}Red and ^{DBCO}Blue-TPP. *S. aureus* were stained with ^{0Az}Red (50 μM) in LB medium for 60 min, washed with PBS and then cultured with or without **^{DBCO}Blue-TPP** (50 μM). After 60 min incubation, *S. aureus* were harvested, washed with PBS three times, maintained in LB medium containing CCCP (0, 300 μM) for 1 h, and then directly analyzed by confocal fluorescence microscopy.

Tagging stressed bacteria *via* BCCL with ^{2AZ}Red and ^{DBCO}Blue-TPP. *S. aureus* were grown in LB medium containing **^{2AZ}Red** (0, 50 μM) for 60 min, and then cultured with **^{DBCO}Blue-TPP** (0, 100 μM) for 1 h in LB medium. These cells were maintained with CCCP (0, 300 μM) for 1 h in LB medium, and then directly analyzed by confocal fluorescence microscopy without washing (to maintain the levels of CCCP during analysis).

Tagging stressed bacteria *via* BCCL with ^{4AZ}Red and ^{DBCO}Blue-TPP. *S. aureus* were grown in LB medium containing **^{4AZ}Red** (0, 50 μM) for 60 min, and then cultured with **^{DBCO}Blue-TPP** (0, 200 μM) for 1 h in LB medium. These cells were maintained with CCCP (0, 300 μM) for 1 h in LB medium, and then directly analyzed by confocal fluorescence microscopy without washing (to maintain the levels of CCCP during analysis).

Tagging stressed bacteria *via* BCCL with ^{6AZ}Red and ^{DBCO}Blue-TPP. *S. aureus* were stained with **^{6AZ}Red** (0, 200 μM) for 60 min, and then with **^{DBCO}Blue-TPP** (0, 300 μM) for 1 h in LB medium. These cells were maintained with CCCP (0, 300 μM) for 1 h in LB medium, and then directly analyzed by confocal fluorescence microscopy without washing (to maintain the levels of CCCP during analysis).

Tagging stressed bacteria with dendritic sensors of varied molecular weight. *S. aureus* were stained with **^{2AZ}Red** (50 μM), **^{4AZ}Red** (50 μM) or **^{6AZ}Red** (200 μM) for 1 h, and then with **^{DBCO}Blue-TPP** (100 μM, 200 μM, 600 μM) for 60 min in LB medium. These cells were maintained with CCCP (0, 300 μM) for 1 h in LB medium, and then directly imaged by confocal fluorescence microscopy without washing (to maintain the levels of CCCP during analysis).

Effects of molecular weight of optical adducts formed *via* BCCL on phagocytosis imaging. *S. aureus* (OD_{600} = 0.05) were grown at 37 °C in LB medium containing FITC-labelled D-lysine

(FITC–D-Lys) (200 μM) until the OD_{600} reached 0.6. The medium was diluted to OD_{600} ∼ 0.3 with fresh medium containing **^{2AZ}Red** (50 μM), **^{4AZ}Red** (50 μM) or **^{6AZ}Red** (200 μM). After 60 min incubation, the cells were harvested by centrifugation, washed with PBS three times, and then resuspended in LB medium containing **^{DBCO}Blue-TPP** (100 μM, 200 μM, 600 μM) respectively. After 1 h incubation, the cells were harvested, washed with PBS three times, and then imaged by confocal fluorescence microscopy. Bone marrow derived macrophages (BMDMs) were incubated with each of the above bacterial samples at 37 °C for 1 h and then probed by confocal fluorescence microscopy.

Tagging stressed bacteria with Den-pH. *S. aureus* were stained with **^{DBCO}Blue-TPP** (300 μM) for 1 h, and then cultured with **^{6AZ}ProRed-TPP** (200 μM) for 1 h in LB medium. After 60 min incubation, the cells were harvested by centrifugation, washed with LB medium, and then resuspended in sodium phosphate buffer of pH 4.0/pH 7.0 containing CCCP (0, 300 μM) for 1 h. The cells were analyzed by confocal fluorescence microscopy.

pH-dependent fluorescence of Den-pH trapped in *S. aureus*. *S. aureus* were stained with **^{DBCO}Blue-TPP** (300 μM) for 1 h, and then cultured with **^{6AZ}ProRed-TPP** (200 μM) for 60 min in LB medium. After 60 min incubation, the cells were harvested by centrifugation, washed with LB medium, resuspended in sodium phosphate buffer (10 mM) of varied pH (pH: 4.0, 5.0, 6.0, 7.0, 8.0) for 1 h, and then imaged by confocal fluorescence microscopy or by flow cytometry (BD FACS Canto II).

Retention of Den-pH within FITC–D-Lys labelled *S. aureus*. *S. aureus* (OD_{600} = 0.05) were grown at 37 °C in LB medium containing FITC–D-Lys (200 μM) until the OD_{600} reached 0.6. These FITC–D-Lys$^+$ *S. aureus* cells were stained with **^{6AZ}ProRed-TPP** (200 μM) for 1 h, and then cultured with **DBCOBlue-TPP** (600 μM). After 60 min incubation, the cells were harvested, washed with PBS three times, and then resuspended in sodium phosphate buffer (10 mM) of pH 7.0 or pH 4.0. The cells were analyzed by confocal fluorescence microscopy.

Signal-on fluorescence imaging of phagocytosis with Den-pH. *S. aureus* (OD_{600} = 0.05) were grown at 37 °C in LB medium containing FITC–D-Lys (200 μM) until the OD_{600} reached 0.6. These FITC–D-Lys$^+$ *S. aureus* cells were grown at 37 °C in LB medium containing **^{6AZ}ProRed-TPP** (200 μM) for 1 h, and then cultured with **^{DBCO}Blue-TPP** (600 μM) for 60 min. Then the cells were harvested and washed with PBS three times. BMDMs were incubated with the above bacterial samples at 37 °C for 1 h and then imaged by confocal fluorescence microscopy.

Inability of Den-pH to tag *S. aureus*. *S. aureus* were stained with Den-pH (200 μM) in LB medium. After 60 min incubation, *S. aureus* were harvested, washed with PBS three times, and then directly analyzed by confocal fluorescence microscopy.

Leakage of ^{6AZ}ProRed-TPP from engulfed bacteria into lysosomes. *S. aureus* (OD_{600} = 0.05) were grown at 37 °C in LB medium containing FITC–D-Lys (200 μM) until the OD_{600} reached 0.6. These FITC–D-Lys$^+$ *S. aureus* cells were stained with **^{6AZ}ProRed-TPP** (200 μM) for 1 h. After 60 min incubation, the cells were harvested by centrifugation and washed with PBS three times. BMDMs were incubated with the above bacterial samples at 37 °C for 1 h and then the resultant macrophages were stained with lysotracker blue (2 μM) for 30 min. The resultant macrophages were washed with PBS three times, resuspended in BMDM culture media, and then probed by confocal fluorescence microscopy.

Lysosomal acidity-triggered red fluorescence in bacteria in phagocytosis. *S. aureus* (OD_{600} = 0.05) were grown at 37 °C in LB medium containing FITC–D-Lys (200 μM) until the OD_{600} was 0.6. These FITC–D-Lys$^+$ *S. aureus* cells were stained with **^{6AZ}ProRed-TPP** (200 μM) for 1 h, and then cultured with **^{DBCO}Blue-TPP** (600 μM) for 60 min. After 60 min incubation, the cells were harvested by centrifugation and washed with PBS three times. BMDMs were incubated with the above bacterial samples at 37 °C for 1 h. After 1 h incubation, BMDM cells were washed with PBS three times and then incubated in BMDM culture media with or without Baf-A1 (50 nM) for 8 h at 37 °C. The resultant macrophages were washed with PBS three times, resuspended in BMDM culture media, and then probed by confocal fluorescence microscopy.

The organelle localization of ^{DBCO}Blue-TPP. BMDMs were incubated with **^{DBCO}Blue-TPP** (5 μM) at 37 °C for 1 h. And then the resultant macrophages were stained with lysotracker green (2 μM) for 1 min. The resultant macrophages were stained with mitotracker deep red (1 μM) for 10 min, washed with PBS three times, resuspended in BMDM culture media, and then probed by confocal fluorescence microscopy.

The organelle localization of Den-pH. BMDMs were incubated with Den-pH (5 μM) at 37 °C for 1 h. And then the resultant macrophages were stained with lysotracker green (2 μM) for 1 min. The resultant macrophages were washed with PBS three times, resuspended in BMDM culture media, and then probed by confocal fluorescence microscopy.

Conflicts of interest

There are no conflicts to declare.

Acknowledgements

This work was supported by grants from NSF China (22177096, 91854106, 21775130). J. H. was supported by grants from NSF China (81788101).

Notes and references

1 G. E. Purdy, R. M. Owens, L. Bennett, D. G. Russell and B. A. Butcher, *Cell. Microbiol.*, 2005, **7**, 1627–1634.

2 I. Lantos, D. P. Virok, T. Mosolygó, Z. Rázga, K. Burián and V. Endrész, *Pathog. Dis.*, 2018, **76**, fty024.

3 S. K. Gogoi, P. Gopinath, A. Paul, A. Ramesh, S. S. Ghosh and A. Chattopadhyay, *Langmuir*, 2006, **22**, 9322–9328.

4 R. İmamoğlu, H. Kudug, D. Duzgun, Y. Ulusu and I. Gokce, *Production of Recombinant Blue Fluorescent Protein (mTagBFP) for Further Researchs in Bioimaging*, 2017.

5 T. C. Vessoni Penna, M. Ishii, O. Cholewa and L. C. De Souza, *Lett. Appl. Microbiol.*, 2004, **38**, 135–139.

6 K. M. Slade, R. Baker, M. Chua, N. L. Thompson and G. J. Pielak, *Biochemistry*, 2009, **48**, 5083–5089.

7 J. Shin, M. Park, C. Kim, H. Kim, Y. Park, C. Ban, J.-W. Yoon, C.-S. Shin, J. W. Lee, Y.-S. Jin, Y.-C. Park, W.-K. Min and D.-H. Kweon, *Sci. Rep.*, 2020, **10**, 10514.

8 Y. Tian, M. Yu, Z. Li, J. Han, L. Yang and S. Han, *Anal. Chem.*, 2015, **87**, 8381–8386.

9 K. Li, Y.-Y. Zhang, G.-Y. Jiang, Y.-J. Hou, B.-W. Zhang, Q.-X. Zhou and X.-S. Wang, *Chem. Commun.*, 2015, **51**, 7923–7926.

10 L. N. Schulte, B. Heinrich, H. Janga, B. T. Schmeck and O. Vázquez, *Angew. Chem., Int. Ed.*, 2018, **57**, 11564–11568.

11 B. Wang, M. Wang, A. Mikhailovsky, S. Wang and G. C. Bazan, *Angew. Chem., Int. Ed.*, 2017, **56**, 5031–5034.

12 H. Chen, S. Li, M. Wu, Kenry, Z. Huang, C.-S. Lee and B. Liu, *Angew. Chem., Int. Ed.*, 2020, **59**, 632–636.

13 S. Greenberg and S. Grinstein, *Curr. Opin. Immunol.*, 2002, **14**, 136–145.

14 L. M. Stuart and R. A. Ezekowitz, *Nat. Rev. Immunol.*, 2008, **8**, 131–141.

15 J. J. Lim, S. Grinstein and Z. Roth, *Front. Cell. Infect. Microbiol.*, 2017, **7**, 191.

16 H. Minasyan, *Immunol. Res.*, 2018, **66**, 271–280.

17 S. Herbst, A. Shah, M. Mazon Moya, V. Marzola, B. Jensen, A. Reed, M. A. Birrell, S. Saijo, S. Mostowy, S. Shaunak and D. Armstrong-James, *EMBO Mol. Med.*, 2015, **7**, 240–258.

18 C. Rosales and E. Uribe-Querol, *BioMed Res. Int.*, 2017, **2017**, 9042851.

19 S. Bedoui, S. von Hörsten and T. Gebhardt, *Peptides*, 2007, **28**, 373–376.

20 J. Černý and I. Stříž, *Clin. Sci.*, 2019, **133**, 1549–1565.

21 R. B. Raybourne and V. K. Bunning, *Infect. Immun.*, 1994, **62**, 665.

22 S. Kenmoku, Y. Urano, H. Kojima and T. Nagano, *J. Am. Chem. Soc.*, 2007, **129**, 7313–7318.

23 A. Beletskii, M. Cooper, P. Sriraman, C. Chiriac, L. Zhao, S. Abbot and L. Yu, *Biotechniques*, 2005, **39**, 894–897.

24 D. A. Drevets and A. M. Elliott, *J. Immunol. Methods*, 1995, **187**, 69–79.

25 D. A. Drevets and P. A. Campbell, *J. Immunol. Methods*, 1991, **142**, 31–38.

26 V. K. Bunning and R. B. Raybourne, *Ann. N. Y. Acad. Sci.*, 1994, **730**, 273–275.

27 Y. Shi, X. Zou, S. Wen, L. Gao, J. Li, J. Han and S. Han, *Autophagy*, 2021, **17**, 1–16.

28 O. Schmidt, N. Pfanner and C. Meisinger, *Nat. Rev. Mol. Cell Biol.*, 2010, **11**, 655–667.

29 C. Esser, N. Ahmadinejad, C. Wiegand, C. Rotte, F. Sebastiani, G. Gelius-Dietrich, K. Henze, E. Kretschmann, E. Richly, D. Leister, D. Bryant, M. A. Steel, P. J. Lockhart, D. Penny and W. Martin, *Mol. Biol. Evol.*, 2004, **21**, 1643–1660.

30 G. Burger and B. F. Lang, *IUBMB Life*, 2003, **55**, 205–212.

31 W. Crielaard, N. P. J. Cotton, J. B. Jackson, K. J. Hellingwerf and W. N. Konings, *Biochim. Biophys. Acta, Bioenerg.*, 1988, **932**, 17–25.

32 J. P. Stratford, C. L. A. Edwards, M. J. Ghanshyam, D. Malyshev, M. A. Delise, Y. Hayashi and M. Asally, *Proc. Natl. Acad. Sci. U. S. A.*, 2019, **116**, 9552.

33 G. L. Archer, *Clin. Infect. Dis.*, 1998, **26**, 1179–1181.

34 D. Pérez-Montarelo, E. Viedma, M. Murcia, I. Muñoz-Gallego, N. Larrosa, P. Brañas, N. Fernández-Hidalgo, J. Gavaldà, B. Almirante and F. Chaves, *Front. Microbiol.*, 2017, **8**, 917.

35 K. Shettigar and T. S. Murali, *Eur. J. Clin. Microbiol. Infect. Dis.*, 2020, **39**, 2235–2246.

36 T. Alebachew, G. Yismaw, A. Derabe and Z. Sisay, *Ethiop. J. Health Sci.*, 2012, **22**, 209–213.

37 M. W. Casewell, *J. Hosp. Infect.*, 1998, **40**(Suppl B), S3–11.

38 S. Roy, S. Santra, A. Das, S. Dixith, M. Sinha, S. Ghatak, N. Ghosh, P. Banerjee, S. Khanna, S. Mathew-Steiner, P. D. Ghatak, B. N. Blackstone, H. M. Powell, V. K. Bergdall, D. J. Wozniak and C. K. Sen, *Ann. Surg.*, 2020, **271**, 1174–1185.

39 R. V. Rasmussen, U. Høst, M. Arpi, C. Hassager, H. K. Johansen, E. Korup, H. C. Schønheyder, J. Berning, S. Gill, F. S. Rosenvinge, V. G. Fowler, Jr., J. E. Møller, R. L. Skov, C. T. Larsen, T. F. Hansen, S. Mard, J. Smit, P. S. Andersen and N. E. Bruun, *Eur. J. Echocardiogr.*, 2011, **12**, 414–420.

40 M. L. Fernández Guerrero, J. J. González López, A. Goyenechea, J. Fraile and M. de Górgolas, *Medicine*, 2009, **88**, 1–22.

41 W. Kogler, M. Omar, D. Zoltowska and S. Sattiraju, *BMJ Case Rep.*, 2020, **13**, e236530.

42 C. Bouchiat, K. Moreau, S. Devillard, J. P. Rasigade, A. Mosnier, T. Geissmann, M. Bes, A. Tristan, G. Lina, F. Laurent, L. Piroth, N. Aissa, X. Duval, V. Le Moing and F. Vandenesch, *Infect., Genet. Evol.*, 2015, **36**, 524–530.

43 T. Bajaj, A. Karapetians, N. Karapetians, H. Duong and A. Heidari, *AME Case Reports*, 2020, **4**, 4, DOI: 10.21037/acr.2019.11.06.

44 H. Strahl and L. W. Hamoen, *Proc. Natl. Acad. Sci. U. S. A.*, 2010, **107**, 12281.

45 E. Kuru, H. V. Hughes, P. J. Brown, E. Hall, S. Tekkam, F. Cava, M. A. de Pedro, Y. V. Brun and M. S. VanNieuwenhze, *Angew. Chem., Int. Ed.*, 2012, **51**, 12519–12523.

46 Z. Xue, H. Zhao, J. Liu, J. Han and S. Han, *ACS Sens.*, 2017, **2**, 436–442.

47 Z. Xue, E. Zhang, J. Liu, J. Han and S. Han, *Angew. Chem., Int. Ed.*, 2018, **57**, 10096–10101.

48 E. Zhang, Y. Shi, J. Han and S. Han, *Anal. Chem.*, 2020, **92**, 15059–15068.

49 E. Zhang, S. Wang, X. Su and S. Han, *Analyst*, 2020, **145**, 1319–1327.

50 T. Yoshimori, A. Yamamoto, Y. Moriyama, M. Futai and Y. Tashiro, *J. Biol. Chem.*, 1991, **266**, 17707–17712.

51 M. A. B. Axelsson, N. G. Karlsson, D. M. Steel, J. Ouwendijk, T. Nilsson and G. C. Hansson, *Glycobiology*, 2001, **11**, 633–644.

52 S. Jin, Y. Hao, Z. Zhu, N. Muhammad, Z. Zhang, K. Wang, Y. Guo, Z. Guo and X. Wang, *Inorg. Chem.*, 2018, **57**, 11135–11145.

53 J. B. Grimm and L. D. Lavis, *Org. Lett.*, 2011, **13**, 6354–6357.